

Supporting information for

**Hydrophilic and strengthened 3D reduced graphene oxide/nano-  
Fe<sub>3</sub>O<sub>4</sub> hybrid hydrogel for enhanced adsorption and catalytic  
oxidation of typical pharmaceuticals**

Danna Shan,<sup>a</sup> Shubo Deng,<sup>\*,a</sup> Chengxu Jiang,<sup>a</sup> Yue Chen,<sup>a</sup> Bin Wang,<sup>a</sup> Yujue Wang,<sup>a</sup>

Jun Huang,<sup>a</sup> Gang Yu<sup>a</sup> and Mark R. Wiesner<sup>b</sup>

<sup>a</sup> School of Environment, Beijing Key Laboratory for Emerging Organic Contaminants Control, State Key Joint Laboratory of Environment Simulation and Pollution Control (SKLESPC), Tsinghua University, Beijing 100084, China

<sup>b</sup> Department of Civil and Environmental Engineering, Duke University, P.O. Box 90287, Durham, NC 27708-0287, USA

\* Corresponding author. Tel: +86-10-62792165. Fax: +86-10-62794006.

E-mail: dengshubo@tsinghua.edu.cn (S. Deng)

**Table S1** Kinetic parameters for the adsorption of CIP and TC on 3D-rGO/Fe<sub>3</sub>O<sub>4</sub>

Adsorbate	Pseudo second-order parameter			R <sup>2</sup>
	<i>k</i> (g/(μmol·h))	q <sub>e</sub> (μmol/g)	ν <sub>0</sub> (μmol/(g·h))	
CIP	0.00026	546.3	77.6	0.979
TC	0.00031	556.7	96.1	0.962

**Table S2** Calculated parameter values of the Langmuir model for CIP and TC adsorption on 3D-rGO/Fe<sub>3</sub>O<sub>4</sub>, 3D-rGO, GO, rGO and EG in the whole concentration range

Adsorbents	Adsorbates	Langmuir model <sup>a</sup>		
		<i>b</i> (L/μmol)	q <sub>m</sub> (mmol/g)	R <sup>2</sup>
3D-rGO/Fe <sub>3</sub> O <sub>4</sub>	CIP	0.005	2.78	0.933
	TC	0.007	4.76	0.989
3D-rGO	CIP	0.018	0.95	0.794
	TC	0.028	0.98	0.983
GO	CIP	3.285	0.52	0.689
	TC	0.142	0.61	0.912
rGO	CIP	7.664	0.21	0.994
	TC	0.316	0.12	0.561
EG	CIP	0.219	0.07	0.880
	TC	0.137	0.08	0.688

<sup>a</sup>  $q_e = q_m C_e / (1/b + C_e)$

**Table S3** Calculated parameter values of the Langmuir model for CIP and TC adsorption on 3D-rGO/Fe<sub>3</sub>O<sub>4</sub>, 3D-rGO, GO, rGO and EG at equilibrium concentrations below 100 μmol/L

Adsorbents	Adsorbates	Langmuir model <sup>a</sup>		
		<i>b</i> (L/μmol)	<i>q<sub>m</sub></i> (μmol/g)	<i>R</i> <sup>2</sup>
3D-rGO/Fe <sub>3</sub> O <sub>4</sub>	CIP	0.116	842.9	0.781
	TC	0.022	1891.6	0.994
3D-rGO	CIP	0.065	596.3	0.937
	TC	0.097	623.8	0.991
GO	CIP	1.599	567.6	0.861
	TC	0.168	557.2	0.973
rGO	CIP	6.178	237.6	0.965
	TC	0.439	115.2	0.913
EG	CIP	0.221	71.2	0.826
	TC	0.143	73.7	0.599

$$^a q_e = q_m C_e / (1/b + C_e)$$

**Table S4** Surface area and pore volume of 3D-rGO/Fe<sub>3</sub>O<sub>4</sub>, 3D-rGO, GO, rGO and EG

Sample	Specific surface area (m <sup>2</sup> /g) <sup>a</sup>	Total pore volume (cm <sup>3</sup> /g) <sup>b</sup>
3D-rGO/Fe <sub>3</sub> O <sub>4</sub>	66.8	0.285
3D-rGO	55.8	0.214
GO	15.0	0.017
rGO	24.1	0.011
EG	123.2	0.097

<sup>a</sup> The specific surface area was calculated by the BET method.

<sup>b</sup> The pore volume was calculated by the DFT method.

**Table S5** Specific surface area and pore volume of different activated carbons

Parameters	AC-1	AAC	CAC	AC-2
SSA (m <sup>2</sup> /g) <sup>a</sup>	930.5	761.3	545.9	323.7
Pore volume (cm <sup>3</sup> /g) <sup>b</sup>	0.597	0.496	0.353	0.353

<sup>a</sup> The specific surface area was calculated by the BET method.

<sup>b</sup> The pore volume was calculated by the DFT method.

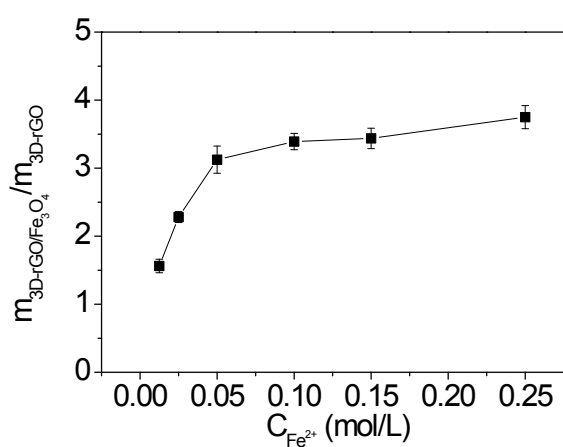


**Fig. S1** Mass ratios of 3D-rGO/Fe<sub>3</sub>O<sub>4</sub> to 3D-rGO prepared at different concentrations of Fe<sup>2+</sup>.

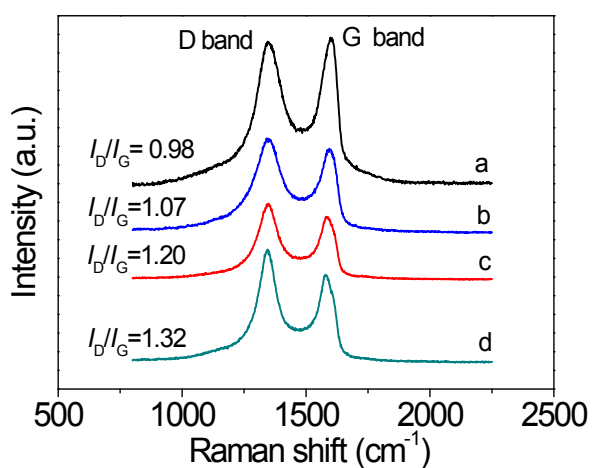


**Fig. S2** Raman spectra of GO (a) and 3D-rGO/Fe<sub>3</sub>O<sub>4</sub> prepared by 0.0125 (b), 0.05 (c) and 0.25 mol/L Fe<sup>2+</sup>(d).

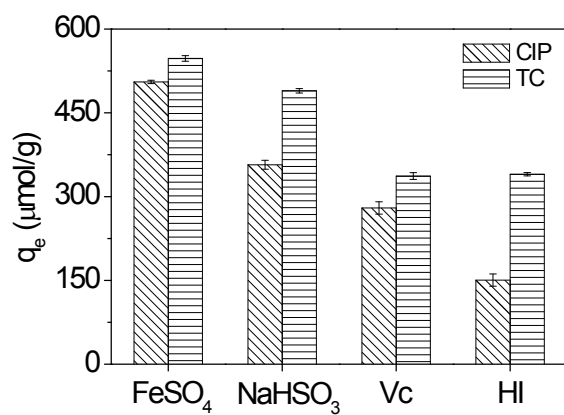


**Fig. S3** Adsorption of CIP and TC on the hydrogels prepared by different reductants.

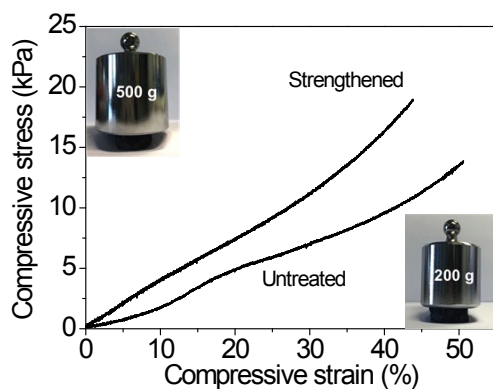


**Fig. S4** Strain-stress curves of untreated and strengthened 3D-rGO/Fe<sub>3</sub>O<sub>4</sub> before and after drying for 1 h.

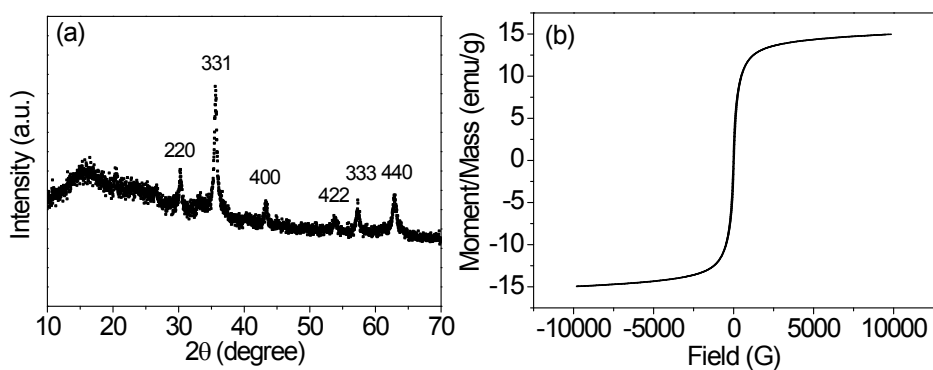


**Fig. S5** XRD pattern (a) and hysteresis curve (b) of 3D-rGO/Fe<sub>3</sub>O<sub>4</sub>.

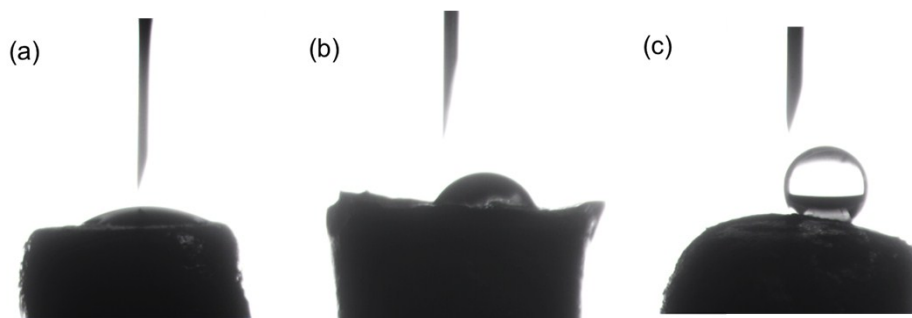


**Fig. S6** Contact angles of 3D-rGO/Fe<sub>3</sub>O<sub>4</sub> (a), 3D-rGO (reduced by NaHSO<sub>3</sub>) (b) and corresponding freeze-dried 3D-rGO (c).

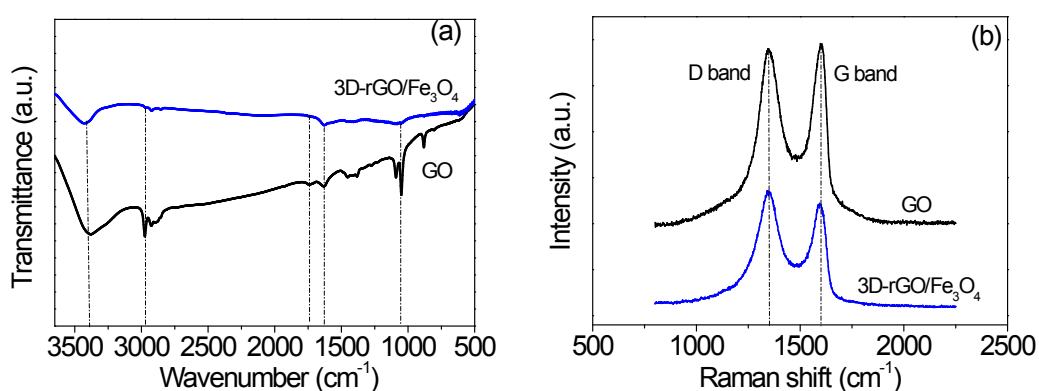


**Fig. S7** FTIR (a) and Raman spectra (b) of GO and 3D-rGO/Fe<sub>3</sub>O<sub>4</sub>.

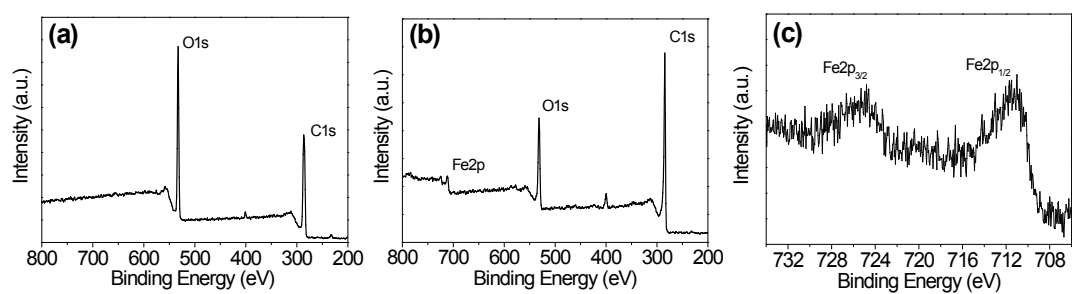


**Fig. S8** XPS spectra of GO (a), 3D-rGO/Fe<sub>3</sub>O<sub>4</sub> (b) and core-level Fe2p spectrum of 3D-rGO/Fe<sub>3</sub>O<sub>4</sub>.

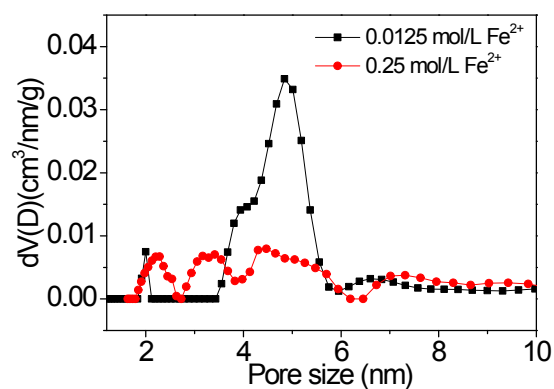


**Fig. S9** Pore size distributions of 3D-rGO/Fe<sub>3</sub>O<sub>4</sub> prepared at 0.0125 and 0.25 mol/L Fe<sup>2+</sup> after 1 h heating.

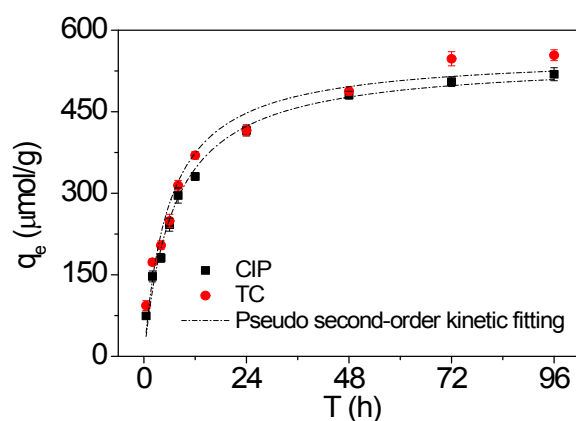


**Fig. S10** Adsorption kinetics of CIP and TC on 3D-rGO/Fe<sub>3</sub>O<sub>4</sub>.

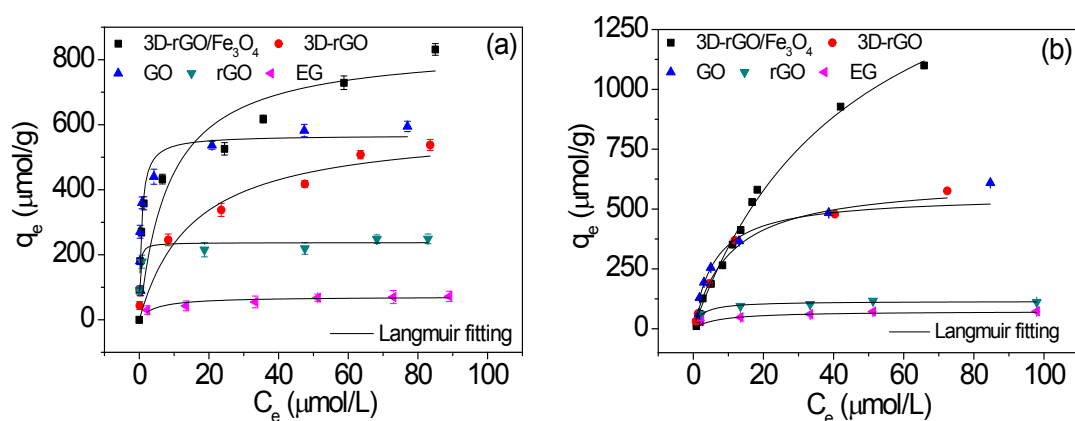


**Fig. S11** Adsorption isotherms of CIP (a) and TC (b) on 3D-rGO/Fe<sub>3</sub>O<sub>4</sub>, 3D-rGO, GO, rGO and EG at the equilibrium concentrations below 100 µmol/L.

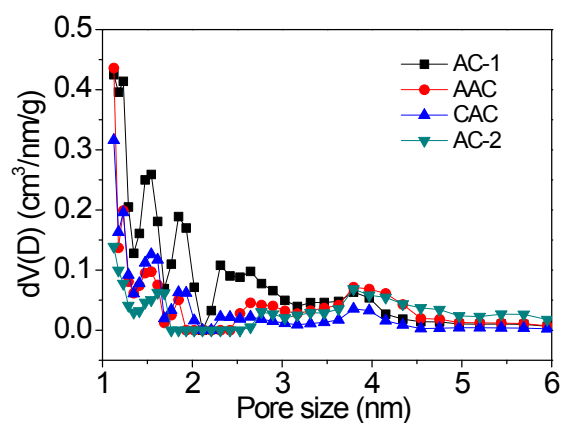


**Fig. S12** Pore size distribution of different ACs.

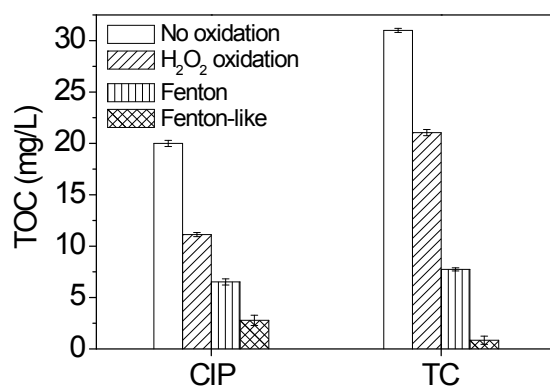


**Fig. S13** TOC concentrations in CIP and TC solutions by Fenton-like (after adsorption), Fenton and  $H_2O_2$  oxidation for 4 h.

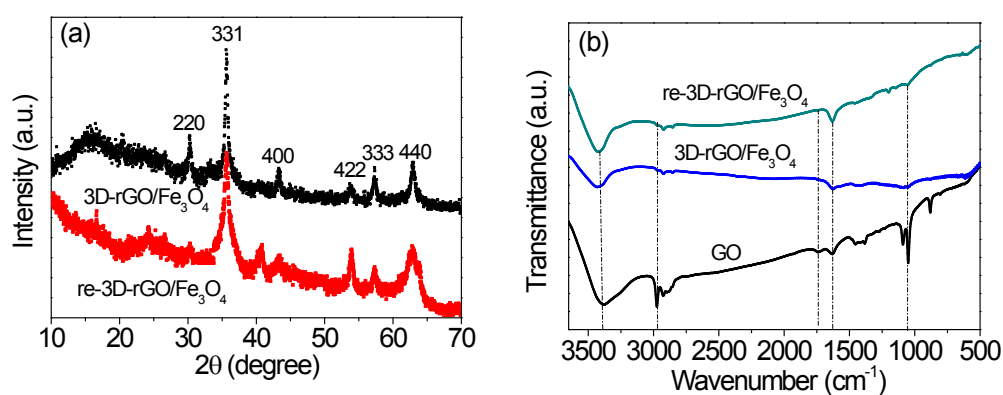


**Fig. S14** XRD patterns of 3D-rGO/ $Fe_3O_4$  and re-3D-rGO/ $Fe_3O_4$  (a), as well as FTIR spectra of GO, 3D-rGO/ $Fe_3O_4$  and re-3D-rGO/ $Fe_3O_4$  (b).



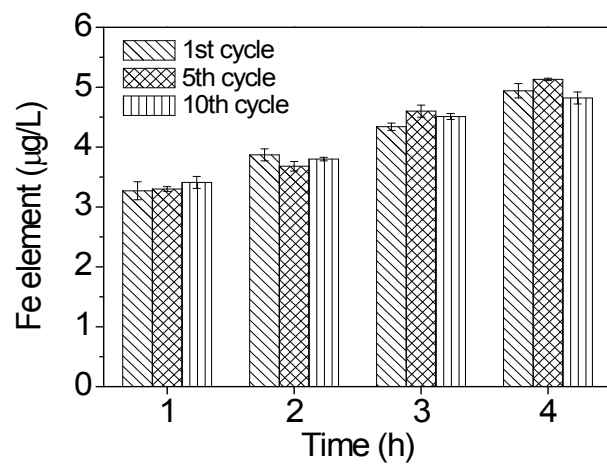


**Fig. S15** Concentration of Fe in solution in the Fenton-like regeneration process.